

Modeling, Simulation and Characterization of Atomic Force Microscopy Measurements for Ionic Transport and Impedance in PEM Fuel Cells

Investigators

Peter M. Pinsky, Professor, Mechanical Engineering; David M. Barnett, Professor, Materials Science and Engineering and Mechanical Engineering; Yongxing Shen, Graduate Researcher.

Introduction

Atomic Force Microscopy (AFM) is an important method for imaging and characterizing the surfaces of fuel cell materials. Such imaging is absolutely essential for understanding why certain designs, selections, and processing of fuel cell membrane materials prove to be successful or unsuccessful choices. In this sense the AFM is currently as crucial to fuel cell technology development as is imaging by electromagnetic and other radiation in modern medicine and health care.

In essence, the AFM is a cantilever beam with a sharp tip which is used to scan a sample of fuel cell membrane material in one of two modes: either intermittently in contact with it or separated from it, as shown in Figure 1. Electronics and control circuits may be used to maintain a fixed tip to sample distance or, say, a constant capacitive force. If the tip-sample interaction can be appropriately modeled, sample surface charge distribution and local surface impedance can be predicted for comparison with experimental measurements and observations. Local impedance measurements are now commonly obtained for purposes of assessing fuel cell membrane quality, but usually using equivalent circuit lump parameter models rather than sound microscopic modeling.

The ability to rationally select and process better fuel cell materials will require a deeper understanding of microscopic mechanistic modeling that currently exists. The purpose of the research described here is to provide an accurate model for quantifying the physics of the AFM tip-sample interactions with the goal of improving the interpretation of AFM measurements of fuel cell membrane local impedance.

Background

The interaction force between an AFM tip and a sample depends on their separation distance and the material properties of both the tip and the sample. Electrostatic forces dominate over van der Waals forces in the situation when the tip-sample separation is on the order of at least a few nanometers. In this regime, the imaging technique is referred to as *Electrostatic Force Microscopy* (EFM). Previous approaches have modeled the problem by approximating the tip geometry as either an object of simpler geometry, such as a sphere or a hyperboloid, or as a member of some family of equipotentials. In both cases approximation errors are introduced. Examples include the metallic tip as a single point charge [1], a series of point charges [2], a sphere [3], a cone [4], a hyperboloid [5], or a cone with a spherical [6] or paraboloid apex [7], where the sample is assumed to be flat and either metallic or homogeneously dielectric [8]. For a sample with surface

roughness, preliminary work has modeled the tip as a sphere [9].

In these works, the tip is always approximated with simplified geometry which may not be accurate for other tip shapes, e.g. pyramid shape. A recent study [10] determines an effective radius of an equivalent spherical apex for arbitrary tip geometry, however, this is based on simple averaging, and does not take into account the built-in horizontal anisotropy of a non-axisymmetric tip. *The current research proposes an accurate model that is based on the actual shape of the AFM tip and circumvents the approximations inherent in existing approaches.*

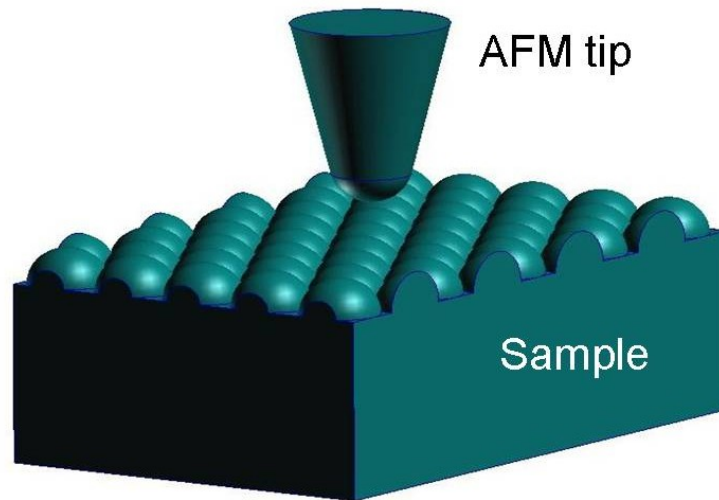


Figure 1: Schematic of the AFM tip, shown without the cantilever support structure, and sample with an idealized surface roughness.

Non-induced (van der Waals) surface charges on the sample surface will induce a force on the AFM tip. *The modeling of interactions of such surface charge distributions with AFM tips has not been addressed in the literature. The current model is capable of modeling the AFM tip interaction arising from arbitrary surface charge distributions.*

Results

In this section we outline our modeling approaches for Electrostatic Force Microscopy and describe results for the following three classes of problems:

1. Capacitance Problem
2. Computation of Coulombic Force Due to Presence of Fixed Sample Charges
3. Quantitative Study of Topographic Effect

1. Electrostatic Force Microscopy Modeling

We start our modeling review by examining the coulombic electric field due to the AFM tip and sample. Since no spatial charge is present in the media between the tip and sample, the electric potential is governed by Laplace's equation,

$$\nabla^2 \phi = 0 \quad (1)$$

where $\nabla^2 = \frac{\partial^2}{\partial x^2} + \frac{\partial^2}{\partial y^2} + \frac{\partial^2}{\partial z^2}$ is the Laplacian operator, x, y, z are the cartesian coordinates, and ϕ is the electric potential (voltage).

The tip and sample serve as boundary conditions and we adopt the assumption of a metallic tip, which is valid for both a bulk metallic tip and a tip with a metallic coating. Hence on the tip surface,

$$\phi = \text{constant} \quad (2)$$

where the absolute value of this constant is immaterial and will be chosen to ease the subsequent computation. No assumption is made for the tip geometry, because virtually any realistic shape of tip surface can be solved by the proposed computational approach.

The specification of the boundary condition associated with the sample plays a crucial role in the modeling, and three types of simplified boundary conditions are discussed in the subsequent subsections.

With the boundary conditions both on the tip surface S_{tip} and the sample surface S_{sam} , as depicted in Figure 2, we are able to solve this boundary value problem and obtain the total force exerting on the AFM tip through

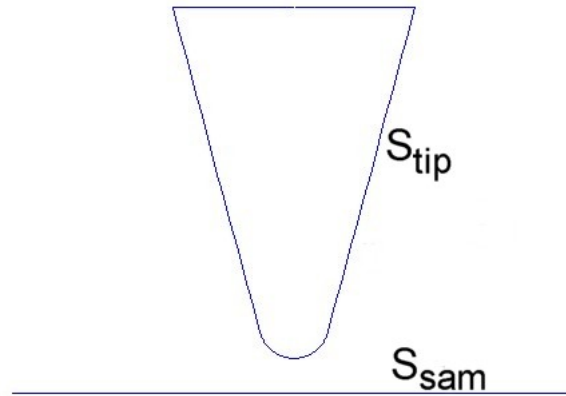


Figure 2: Schematic graph of the boundaries of the boundary value problem

$$F_\alpha = \int_{S_{\text{tip}}} \sum_{\beta=1}^3 T_{\alpha\beta} n_\beta dA \quad (3)$$

where

$$T_{\alpha\beta} = \epsilon_0 (E_\alpha E_\beta - \frac{1}{2} \mathbf{E} \cdot \mathbf{E} \delta_{\alpha\beta}) \quad (4)$$

are the components of the Maxwell stress tensor [11], \mathbf{n} the outer surface normal of the tip, ϵ_0 the permittivity of vacuum, and $\mathbf{E} = -\nabla\phi$ the electric field.

Noticing the fact that \mathbf{E} only has its normal component on S_{tip} , (3) reduces to

$$F_\alpha = \int_{S_{\text{tip}}} \frac{\sigma^2}{2\epsilon_0} n_\alpha dA \quad (5)$$

where

$$\sigma = -\varepsilon_0 \frac{\partial \phi}{\partial n} \quad (6)$$

is the surface charge density on S_{tip} .

2. Capacitance Problem

In the case when we have a metallic sample (for example, gold) whose surface is flat and much larger than the conical part of the tip, both the tip and the sample are held at constant but different potentials. Without loss of generality, we assume the sample is grounded, and the tip is at unit potential, we then have boundary conditions as

$$\begin{cases} \phi = 1 & \text{on } S_{\text{tip}} \\ \phi = 0 & \text{on } S_{\text{sam}} \end{cases} \quad (7)$$

In our 2005 GCEP report [12], we derived a boundary integral equation

$$\int_{S_{\text{tip}}} G(\mathbf{x}, \mathbf{x}') \sigma(\mathbf{x}) dS(\mathbf{x}) = 1, \quad \forall \mathbf{x}' \in S_{\text{tip}} \quad (8)$$

where $G(\mathbf{x}, \mathbf{x}')$ is the half-space electrostatic Green's function that satisfies

$$\begin{cases} -\nabla^2 G(\mathbf{x}, \mathbf{x}') = \delta(\mathbf{x} - \mathbf{x}') \\ G(\mathbf{x}, \mathbf{x}') = 0, \quad \forall \mathbf{x}' \in S_{\text{sam}} \end{cases} \quad (9)$$

with $\delta(\mathbf{x} - \mathbf{x}')$ the Dirac delta function.

A variational approach has been established to solve (8); details are omitted here. Plots of results for a 2D model problem of the tip-sample interaction, including comparison with some previously published models, are shown in Figure 3. It can be seen that the proposed model agrees with the solution whereby the tip is replaced by a cylinder of the same size (the magenta curve in Figure 3(a)) for large tip-sample separation, in which case the actual geometry of the tip is immaterial. On the other hand, our model also converges to the force given by a cylinder with the same curvature of the tip apex placed at the same separation (the black curve in Figure 3(b)) when the tip is very close to the sample, which is reasonable because in this regime, the force is dominated by the tip apex curvature.

In order to investigate multiple computational schemes, we have also employed finite element analysis (FEA) to directly solve the boundary value problem defined by (1) and (7) in 3D. A comparison plot of experimental results, FEA prediction, and predictions of several external approaches are given in Figure 4, which shows excellent agreement of the predicted and measured forces.

3. Computation of Coulombic Force Due to Presence of Fixed Sample Charges

Another case of interest is when we have a dielectric sample whose surface has a distribution of fixed charges $\sigma_0(\mathbf{x})$. In this case, the boundary condition for S_{sam} becomes

$$\varepsilon_0 \frac{\partial \phi}{\partial \mathbf{N}}(\mathbf{x}) = \sigma_0(\mathbf{x}), \quad \forall \mathbf{x} \in S_{\text{sam}} \quad (10)$$

where \mathbf{N} is the outer normal of the computational domain (air) at the sample surface, hence pointing towards the sample. The counterpart of (8) becomes,

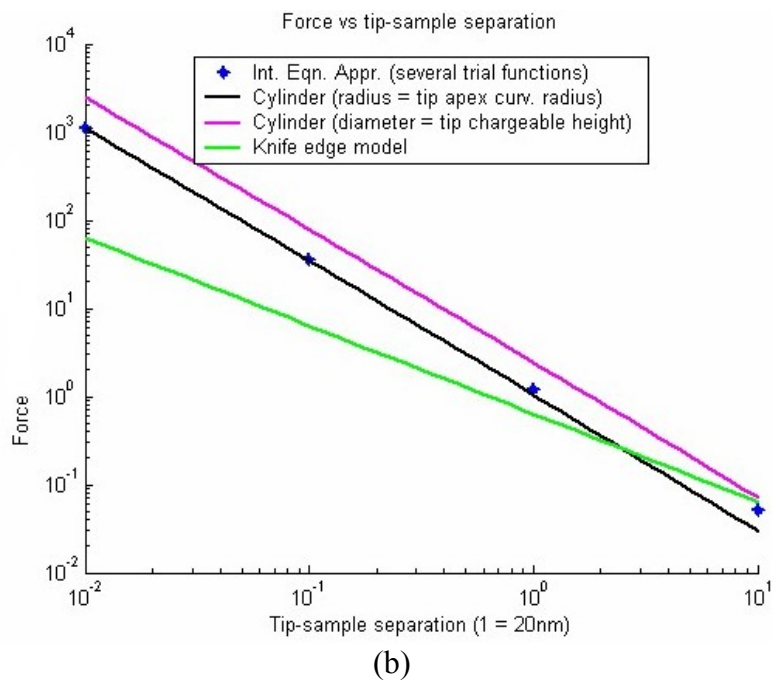
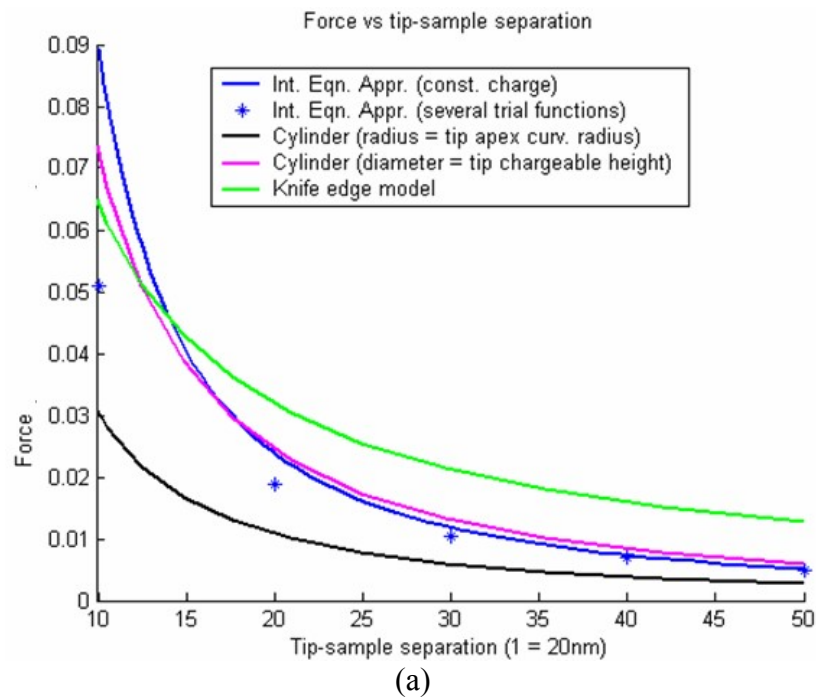


Figure 3: Plots of force vs separation for capacitance problems in 2D. The curves labeled “Int. Eqn. Appr.” is our approach. For fair comparison, the other models are selected as 2D equivalents of some 3D models. The tip apex curvature radius is 20nm. The cone angle of the tip is 30 degrees. (a) is for large separation and (b) is for small separation. Notice (b) is a log-log plot.

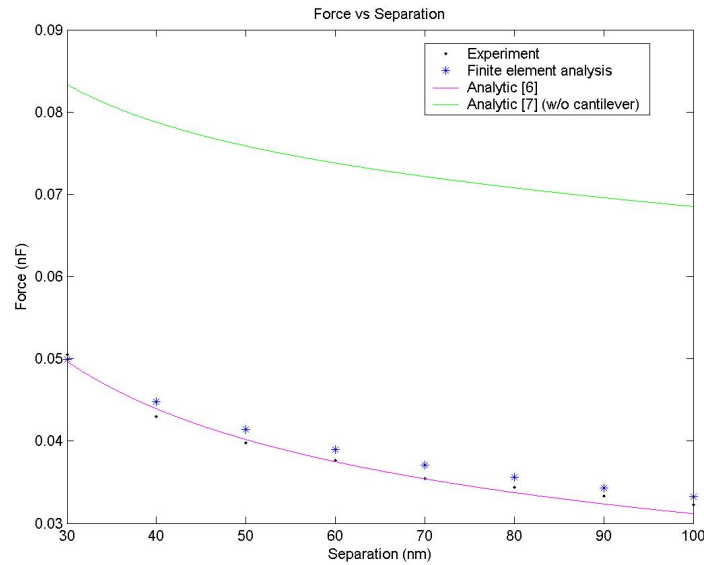


Figure 4: Plot of force vs separation in 3D capacitance problem. The bias between the tip and the sample is set to be 1V. The experimental results are based on amplitude measurements [13].

$$\int_{S_{\text{tip}}} \bar{G}(\mathbf{x}, \mathbf{x}') \sigma(\mathbf{x}) dS(\mathbf{x}) = -I(\mathbf{x}'), \quad \forall \mathbf{x}' \in S_{\text{tip}} \quad (11)$$

where $\sigma(\mathbf{x})$ is, again, the unknown surface charge density on S_{tip} , $\bar{G}(\mathbf{x}, \mathbf{x}')$ is the Green's function that satisfies

$$\begin{cases} -\nabla^2 \bar{G}(\mathbf{x}, \mathbf{x}') = \delta(\mathbf{x} - \mathbf{x}') \\ \frac{\partial}{\partial N} \bar{G}(\mathbf{x}, \mathbf{x}') = 0, \forall \mathbf{x}' \in S_{\text{sam}} \end{cases} \quad (12)$$

and

$$I(\mathbf{x}') = \int_{S_{\text{sam}}} \bar{G}(\mathbf{x}, \mathbf{x}') \sigma_0(\mathbf{x}) dS(\mathbf{x}) \quad (13)$$

For a flat sample with simple (such as sinusoidal) charge distributions we have analytic expressions for $I(\mathbf{x}')$.

Using the similar methods developed in section 2, we have solved this boundary value problem and calculated the tip force by virtue of (5) in the cases where we have a sample with (a) sinusoidal surface charge distribution, (b) equally spacing concentrated charges with equal magnitudes and alternating signs, (c) equally spacing concentrated dipoles. We find that all these surface charge distribution would result in a sinusoidal force map as the tip scans horizontally above the sample (except in case (b) or (c) when the separation is within than 0.4 times the charge periodicity), whereas the force decays exponentially as the tip displaces away from the sample. Figure 5 shows this exponential dependence.

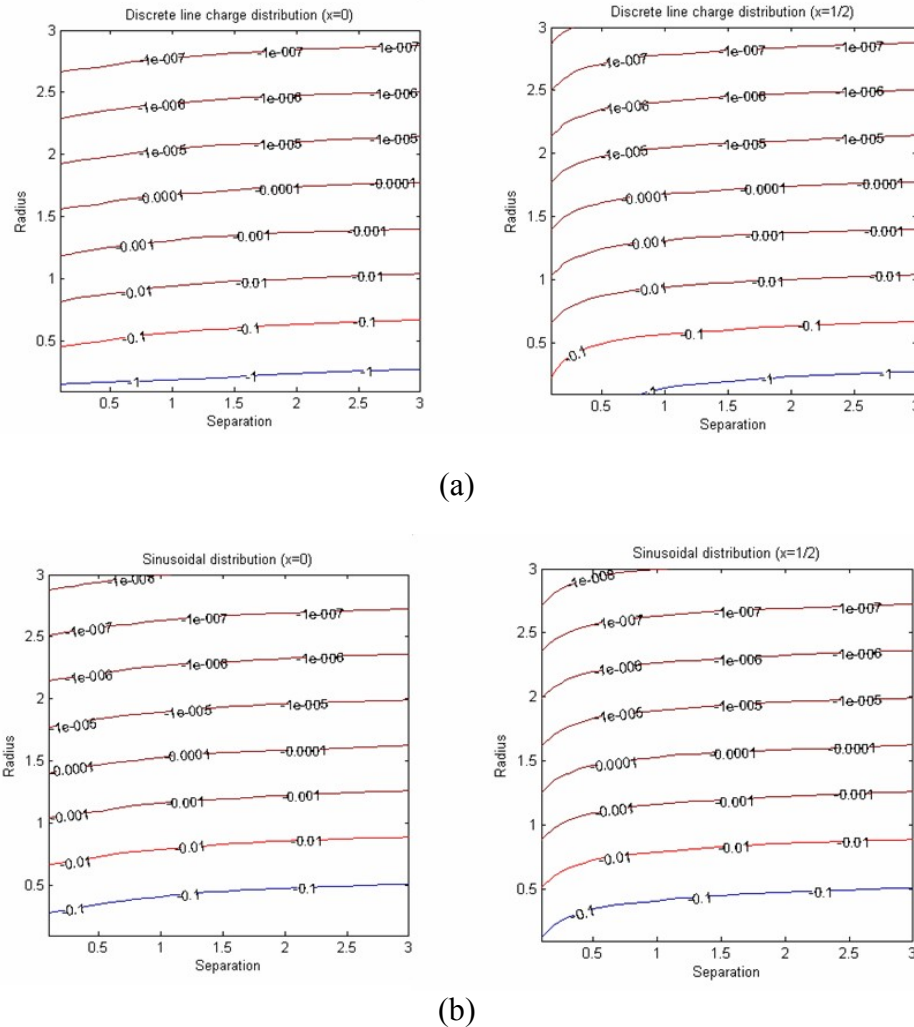


Figure 5: Contour maps of maximum (on the left) and minimum (on the right) forces vs tip apex radius and tip-sample separation as the tip scans horizontally above the sample with (a) discrete line charges, (b) sinusoidal charge distribution. The calculations are set up in 2D. All the numbers are non-dimensional.

Since we are able to model the force for a sinusoidal surface charge distribution, we are now also able to calculate the force for virtually any distribution of sample surface charge, by means of Fourier series or Fourier transform and term-by-term calculation. This also sheds some light to the inverse problem of extracting sample charge distribution from the force map.

4. Quantitative Study of Topographic Effect

We have been assuming the sample to have a flat surface. In reality, this is not always the case. Hence we have also modeled the effect on the tip force due to roughness of the sample surface.

If we have a rough sample, the experiment is usually performed in a two-scan fashion. First, use contact mode or intermittent mode to get the sample topography based on constant force feedback, where the van der Waals force dominates the total force; second, perform EFM measurements by interleaving the tip to maintain a constant “separation” above the sample to suppress the noise due to sample roughness. Now *separation* here means the maximum distance that the tip can move vertically downward without penetration, as shown in Figure 6.

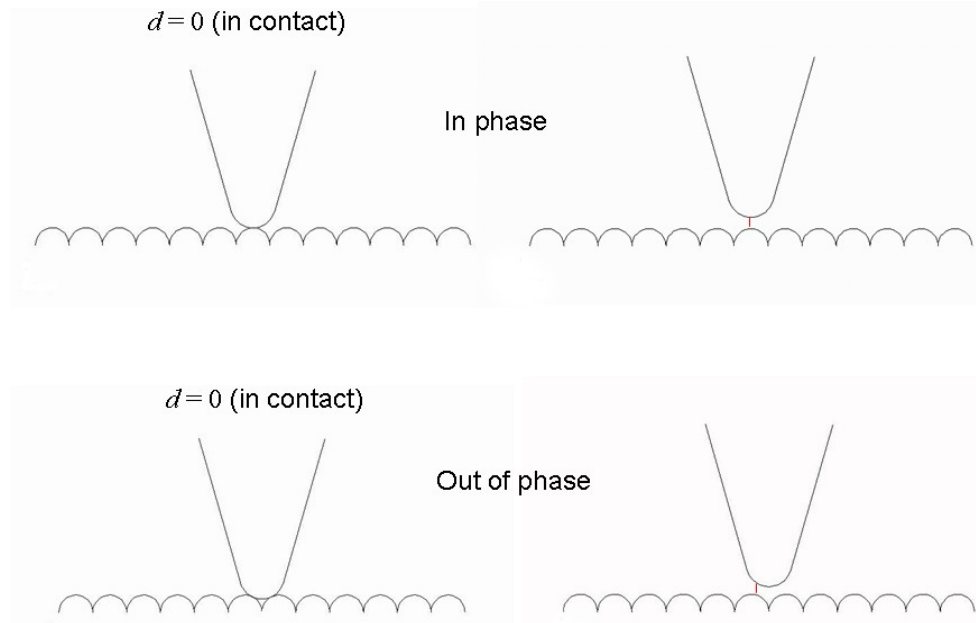


Figure 6: Definition of tip-sample separation d for rough samples. Non-zero separations are depicted by red line segments in the upper and lower right figures.

We have set up a model calculation in 2D to study the topographic effect on the charge measurement. To isolate the effect only due to topography, we assume the sample is at constant potential and has periodic “bumps” made of circular arcs. We then let the tip scan over the sample while maintaining a constant separation defined above, and register the forces that the tip would sense. The force calculation is shown in Figure 7. The fact that this calculated force respects the periodicity of the sample topography indicates the validity of the modeling.

Whether the topographic effect is large enough to affect the charge measurement is yet to be concluded, since our computation tool is not yet able to couple these two effects.

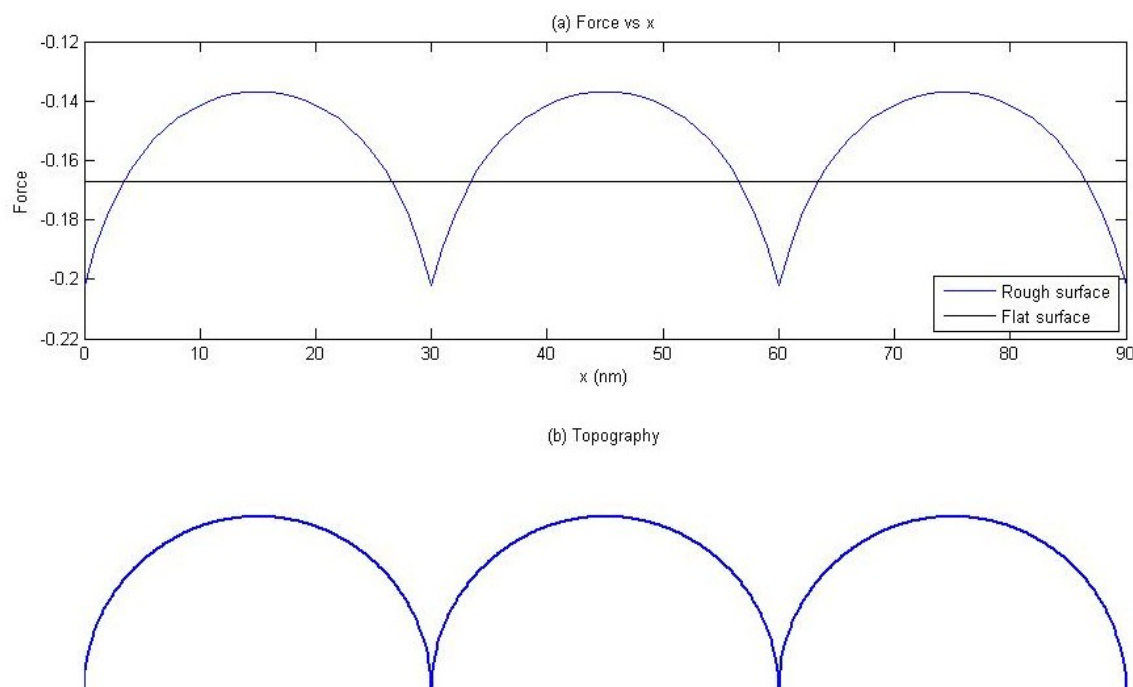


Figure 7: (a) Model calculation of force measurement on rough surface. The tip is maintained at a constant interleave distance above the sample. Negative forces indicate that the tip is attracted to the sample. (b) The corresponding surface topography.

Progress

In this project we are examining and characterizing the properties of solid polymer membranes through analytical and numerical modeling. To address the challenges of enabling new solid polymer fuel cell membranes, the project has set four primary objectives:

1. *AFM imaging.* Nanoscale AFM surface imaging of dielectric or polarizable fuel cell materials involves complex AFM tip interactions with unknown surface and space charges resulting in electrostatic and van der Waals forces. Modeling will be employed to solve the inverse problem of finding the charge distributions from AFM images with the goal of elucidating the mechanisms of charge motion in fuel cell and biological media relevant for environmental cleanup.
2. *Simulation of impedance measurements.* Modeling and simulation of AFM impedance measurements in fuel cells to shed light on the effects of probe tip geometry and surface roughness and topography with goal of developing scaling laws for fuel cell performance.
3. *Modeling of ionic transport in PEMFC's.* Analytical and numerical modeling of ionic diffusion in fuel cells taking into account electrochemical kinetics, current distribution, hydrodynamics and multi-component transport with goal of elucidating mass transport characteristics.

4. *Particle diffusion modeling.* In order to further understand mechanisms of ion and solvent transport in hydrated PEMFC membranes, novel modeling that accounts for local molecular information will be employed.

To date, we have focused primarily on Objective 1. We have developed computational models to predict the EFM measurements on fuel cell membranes, taking into account the contribution from both the sample surface charge distribution and topography. The new solution approaches provide accurate solutions for wide variations in the AFM tip-sample separation and the tip apex curvature values. The methods also apply to a dielectric sample with prescribed charge distribution. For the capacitance problem where other models are well-developed, our own calculations agree with both experiments and other analytic models. For the cases where the sample has surface charges or roughness, our models show self-consistency and validity, and are not far from comparability with experiments, provided the 3D counterparts are developed. The latter extension will enable us to quantify the properties of fuel cell membranes and evaluate their quality based on EFM measurements.

Future Plans

1. *3D extension of computational framework*
Extending our models for charged or rough samples from 2D to 3D.
2. *Impedance measurements simulation*
Modeling the impedance measurements involved in fuel cell characterization.
3. *Transport through fuel cell*
Modeling ion transports through PEM fuel cells.

Publications

1. Y. Shen, D.M. Barnett and P.M. Pinsky, "Precise modeling of AFM tip-sample interactions: capacitance and capacitive force computations," in preparation.
2. Y. Shen, D.M. Barnett and P.M. Pinsky, "Topographics effects on charge measurements by electrostatic force microscopy," in preparation.

References

1. Hu, J., Xiao, X.-D., Ogletree, D. F., and Salmerón, M., Imaging the condensation and evaporation of molecularly thin films of water with nanometer resolution, *Science* 268 (5208), 267-269, 1995.
2. Belaidi, S., Girard, P., and Leveque, G., Electrostatic forces acting on the tip in atomic force microscopy: Modelization and comparison with analytic expressions, *J. Appl. Phys.* 81 (3), 1023-1030, 1997.
3. Terris, B. D., Stern, J. E., Rugar, D., and Mamin, H. J., Contact electrification using force microscopy, *Phys. Rev. Lett.* 63 (24), 2669-2672, 1989.
4. Yokoyama, H., Inoue, T., and Itoh, J., Nonresonant detection of electric force gradients by dynamic force microscopy, *Appl. Phys. Lett.* 65(24), 3143-3145, 1994.
5. Hao, H. W., Baró, A. M., and Sáenz, J. J., Electrostatic and contact forces in force microscopy, *J. Vac. Sci. Technol. B* 9(2), 1323-1328, 1991.
6. Hudlet, S., Saint Jean, M., Guthmann, C., and Berger, J., Evaluation of the capacitive force between an atomic force microscopy tip and a metallic surface, *Eur. Phys. J. B* 2, 5-10, 1998.

7. Colchero, J., Gil, A., and Baró, A. M., Resolution enhancement and improved data interpretation in electrostatic force microscopy, *Phys. Rev. B* 64, 245403, 2001.
8. Gómez-Moñivas, S., Froufe-Pérez, L. S., Caamaño, A. J., and Sáenz, J. J., Electrostatic forces between sharp tips and metallic and dielectric samples, *Appl. Phys. Lett.* 79 (24), 4048-4050, 2001
9. Boyer, L., Houzé, F., Tonck, A., Loubet, J.-L., and Georges, J.-M., The influence of surface roughness on the capacitance between a sphere and a plane, *J. Phys. D* 27, 1504-1508, 1994.
10. Sacha, G. M., Verdaguer, A., Martínez, J., Sáenz, J. J., Ogletree, D. F., Salmeron, M., Effective tip radius in electrostatic force microscopy, *Appl. Phys. Lett.* 86, 123101, 2005.
11. See, for example, Jackson, J. D., *Classical electrodynamics*, Third Edition, John Wiley & Sons, Inc., 1998.
12. Pinsky, P. M., Barnett, D. M., Shen, Y., Modeling, simulation and characterization of atomic force microscopy measurements for ionic transport and impedance in PEM fuel cells, GCEP progress report, 2005.
13. Lee, W., personal correspondence.

Contacts

Peter M. Pinsky: pinsky@stanford.edu

David M. Barnett: barnett@stanford.edu